Send Orders for Reprints to reprints@benthamscience.net

The Open Superconductors Journal, 2013, *4*, 1-23

Open Access

Limiting Factors for Stable Operating Conditions of 1G and 2G High-T_c Superconducting Current-Carrying Elements in High Magnetic Fields

V.R. Romanovskii[a,*], K. Watanabe[c], A.M. Arkharov[b], S. Awaji[c], N.A. Lavrov[b] and V.K. Ozhogina[a]

[a]*NBIKS-Center, National Research Center 'Kurchatov Institute', Moscow 123182, Russia*

[b]*Moscow State Bauman Technical University, 107005 2nd Bauman Str., 5, Moscow, Russia*

[c]*High Field Laboratory for Superconducting Materials, Institute for Materials Research, Tohoku University, Sendai 980-8577, Japan*

Abstract: The limiting currents stably flowing in the current-carrying elements based on 1G and 2G high-temperature superconductors (HTS) are studied. An analysis of the stability of macroscopic thermal and electrical states in the current charging modes is made in terms of the static zero-dimensional and one-dimensional models. For the coated tapes based on the $YBa_2Cu_30_7$ (Y123), the stability investigation was made varying the thicknesses of the copper or silver, external magnetic field and cooling conditions. The analysis performed reveals that the currents of the instability do not practically depend on the thicknesses of copper or silver when the superconducting current-carrying element made of the Y123 is cooled by the cryocooler. At the same time, the increase in the thickness of the stabilizing copper layer leads to a monotonic increase in the limiting stable currents, if the liquid helium (LHe) is used as a coolant. The mechanisms of these features are discussed. It is shown that the limiting stable currents and the induced electric fields depending on the cooling conditions can be both below (subcritical regime) and above (overcritical regime) of a priori defined critical values of the electric field and current of superconductor. The stability criteria of DC regimes are written for the superconducting wires, which structurally consist of superconducting multi-filaments placed into a non-superconducting matrix. They permit one to estimate the allowable limiting values of the charged current, the induced electric field and the overheating of superconductor, which can lead to both the subcritical and overcritical stable regimes. The boundary conditions of them are formulated. In particular, the peculiarities of the stable limiting current regimes of Ag-sheathed $Bi_2Sr_2CaCu_2O_8$ (Bi2212/Ag) wire are discussed in detail. As a result, the investigation performed extends significantly the class of admissible states of HTS as it proves the existence of stable resistive modes in which they do not go to the normal states in spite of the overcritical operating states that take place under different cooling conditions.

Keywords: High-temperature superconductors, voltage-current characteristic, current instability, overheating, flux creep.

1. INTRODUCTION

It is important to make the physical measurements in a high static magnetic field for many applications. Static magnetic fields can be generated by resistive coils. However, these coils consume too much energy and, thus, require intensive water cooling. For example, if to produce 10T the water-cooled resistive magnet is only used, the consumption of electrical energy will be more megawatts. To generate higher magnetic field, the resistive water-cooled magnet will require tens of megawatts [1]. On the other hand, even the hybrid superconducting magnet of 20 T, one of whose sections is made of a superconductor, can be powered by DC that leads to several tens of kilowatts [2], which is essentially less of the energy consumption with a resistive water-cooled magnet. Therefore, for generation of the magnetic fields higher than 20 T, the hybrid coils with several sections are preferable. Moreover, the purely superconducting magnets can allow indefinitely measurements in ultrahigh magnetic fields to be made. These superconducting magnets raise the qualitative level of the physics researches of semiconductors, metals or superconducting materials, as well as magnetic resonance imaging or biological studies.

Progress in the production of superconducting materials enables creation of very high magnetic fields. It is now possible to obtain a magnetic field with the induction of about 30 T working at the LHe temperature and having when only superconducting sections with HTS inserts. These materials offer a huge advantage as such magnetic fields are unattainable for low-temperature superconductors, and the water-cooled Bitter magnet is unacceptably expensive in operation.

One of the main characteristics of superconductors is the limiting current that can be charged without its transition to the normal state. It corresponds to the maximum stable current load, which is suitable for the superconducting coil. The existence of the limiting current is a direct consequence of the flux creep when finite voltage appears inside the superconductor long before the onset of the instability in the current charging, and, hence, there is a constant heat generation. As a result, the distribution of electric field and

*Address correspondence to this author at the NBIKS-Center, National Research Center 'Kurchatov Institute', Moscow 123182, Russia;
Tel: 7-499-1967955; Fax: 7-499-1965973;
E-mail: vromanovskii@netscape.net

1876-5378/13 2013 Bentham Open

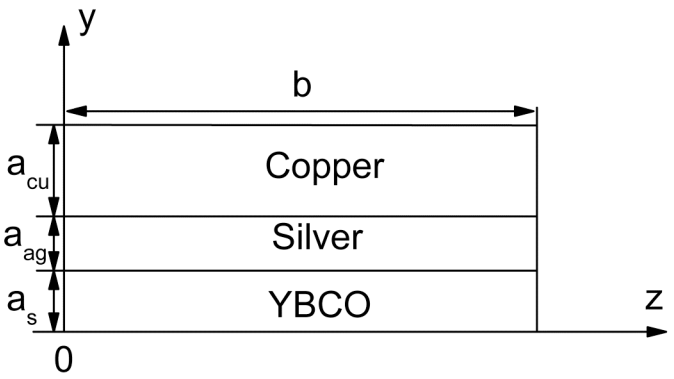

Fig. (1). Schematic view of a current-carrying element based on Y123.

current in the superconductor may become unstable and it may return to the normal state. Therefore, the investigation of the limiting current-carrying capacity of the HTS is important for both the characterization of the performances of them and the understanding of the macroscopic mechanisms limiting their current-carrying capacity taking into consideration the flux creep states.

In this paper, the current-carrying properties of 1G and 2G HTS placed in the high magnetic field are investigated in detail. This study permits the criteria which not only define the limiting stable values of the charged currents in various operating regimes to be formulated but also shows that a priory fixed electric field criterion and the corresponding value of the current have no meaning of the critical quantities. Consequently, the results discussed below made it possible to prove that it is reasonable to use 1G and 2G HTS in the resistive modes charging high operational currents, which may exceed the critical ones.

2. CURRENT STABLITY BOUNDARY OF COATED SUPERCONDUCTING TAPES UNDER DIFFERENT COOLING CONDITIONS

Discovery of Y123 allows developing a new generation of current-carrying elements for many practical applications as their unique critical properties are maintained in very high magnetic fields. Currently, fabrication of long-length Y123-coated tapes stabilized by silver and copper layers meets the real practical requirements. Therefore, the superconducting sections made on the basis of Y123-tape have been already used successfully for creation of coils with high magnetic field.

To ensure the operating temperature of such magnets, the LHe or, otherwise, the conduction-cooling (indirect) method can be used. The latter can be provided with a cryocooler, when the cooling conditions of the superconducting coil do not require cryogen liquid. Cryogen-free superconducting magnets have significantly extended the range of practical applications of superconductivity allowing compact devices to be made. Besides, they possess undeniable advantages. Their ongoing operating costs have been significantly reduced because they only serve for power supply. As a result, the procedure for their start-up and operation is simplified and the technical needs requiring the use of cryogen liquids are eliminated. Accordingly, the problems of safe operation of cryogen-free magnets are not relevant. Therefore, the development of cryogen-free superconducting magnets has received considerable attention [2-8].

The estimation of the limiting current capability of the Y123-based superconducting tapes deposited on a Hastelloy substrate with stabilizing silver and copper coatings is made in sections 2.2 and 2.3 under different cooling conditions on its surface. The investigation is focused on the study of the effect of the coating thicknesses (copper or silver) on the current-carrying capacity of Y123-tapes. This study was made for investigating the fact of the current redistribution between sections in multi-section magnets used for generation of high magnetic fields. In turn, this process may be accompanied by premature transition of the inner Y123-section to the normal state when the induced current exceeds the current stability boundary. Therefore, the problem of a stable current load of Y123-tape must be solved even in the stage of designing superconducting coils.

2.1. Zero-Dimensional Model of Coated Superconducting Tape

Consider the current charging in an infinitely long cooled superconducting tape (Fig. **1**) with a width b consisting of a superconductor with thickness of a_s and stabilizing silver and copper coatings with thicknesses a_{ag} and a_{cu}, respectively, taking into account that $b >> a = a_s+a_{ag}+a_{cu}$. Assume that the time of current charging is sufficiently long; there are no external thermal disturbances; conductive heat flow in the cross section of the tape is much greater than the heat flow to the coolant and, thereby, non-uniformity of temperature and electric field over the cross section and length of the tape is negligible. Formally, this corresponds to the current charging into the tape with highly conducting coatings at an infinitesimal rate. Let us also assume that the critical current density of the superconductor $J_c(T,B)$ is non-linearly dependent on the temperature and magnetic field; the voltage-current characteristic of a superconductor satisfies the power equation with n-value depending on the temperature and magnetic field; the constant external magnetic field has completely penetrated into the tape and its variation in the longitudinal direction can be neglected; transport current flows across the tape with cross section area $S = ab$ and self-field is small in comparison with the external magnetic field; the heat exchange takes place on the surface of the tape with a coolant having temperature T_0 and the cooling perimeter p is $p = \gamma p_0$, where $p_0 = 2(a+b)$ and $0 < \gamma < 1$.

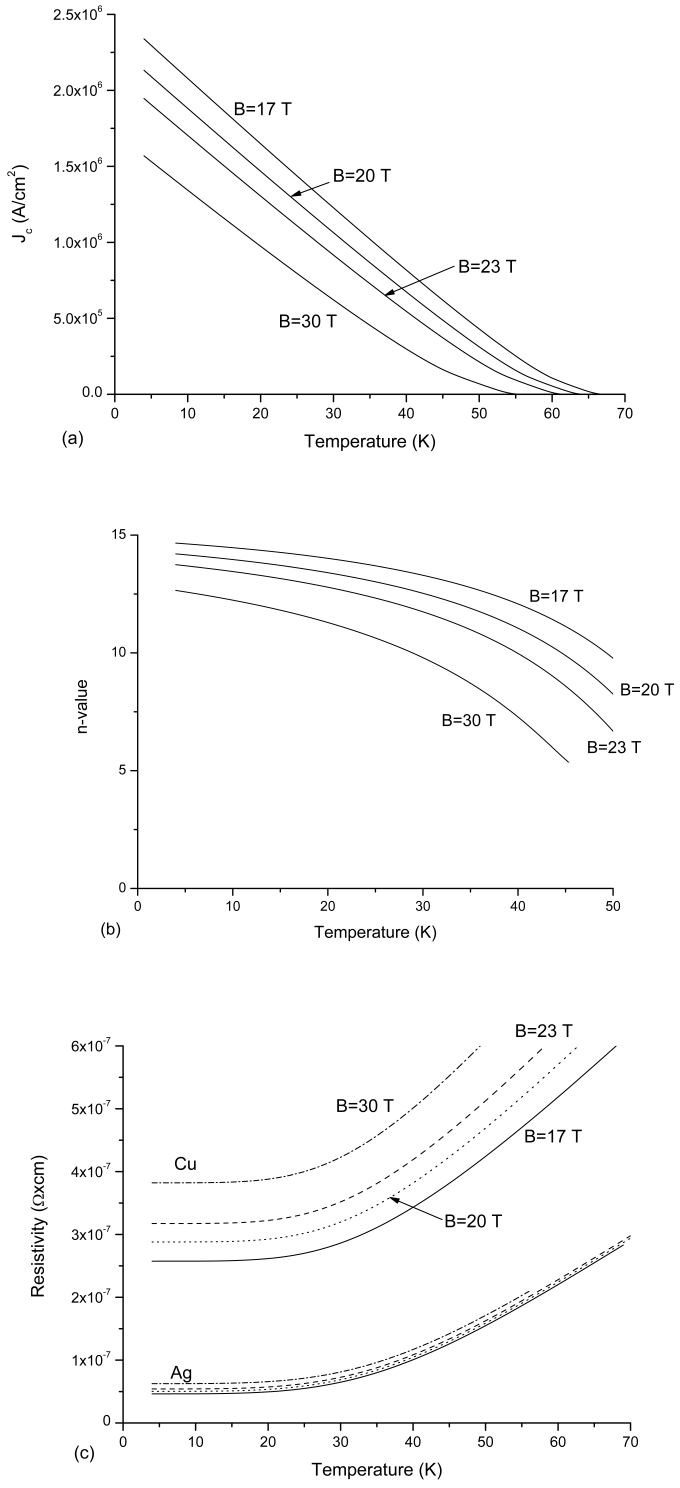

Fig. (2). The dependence of the properties of the superconductor and stabilizing coating on the temperature in different magnetic field.

According to these assumptions, the macroscopic thermal and electrical states of the superconducting tape can be investigated on the basis of a zero-dimensional anisotropic continuum model. Therefore, let us determine the temperature T and the electric field E for the given current density J solving the following system of the static equations

$$EJ = q\left(T\right) p / S, \tag{1}$$

$$E = E_c \left(\frac{J_s}{J_c(T,B)} \right)^{n(T,B)} = J_{ag}\rho_{ag}(T,B) = J_{cu}\rho_{cu}(T,B) \tag{2}$$

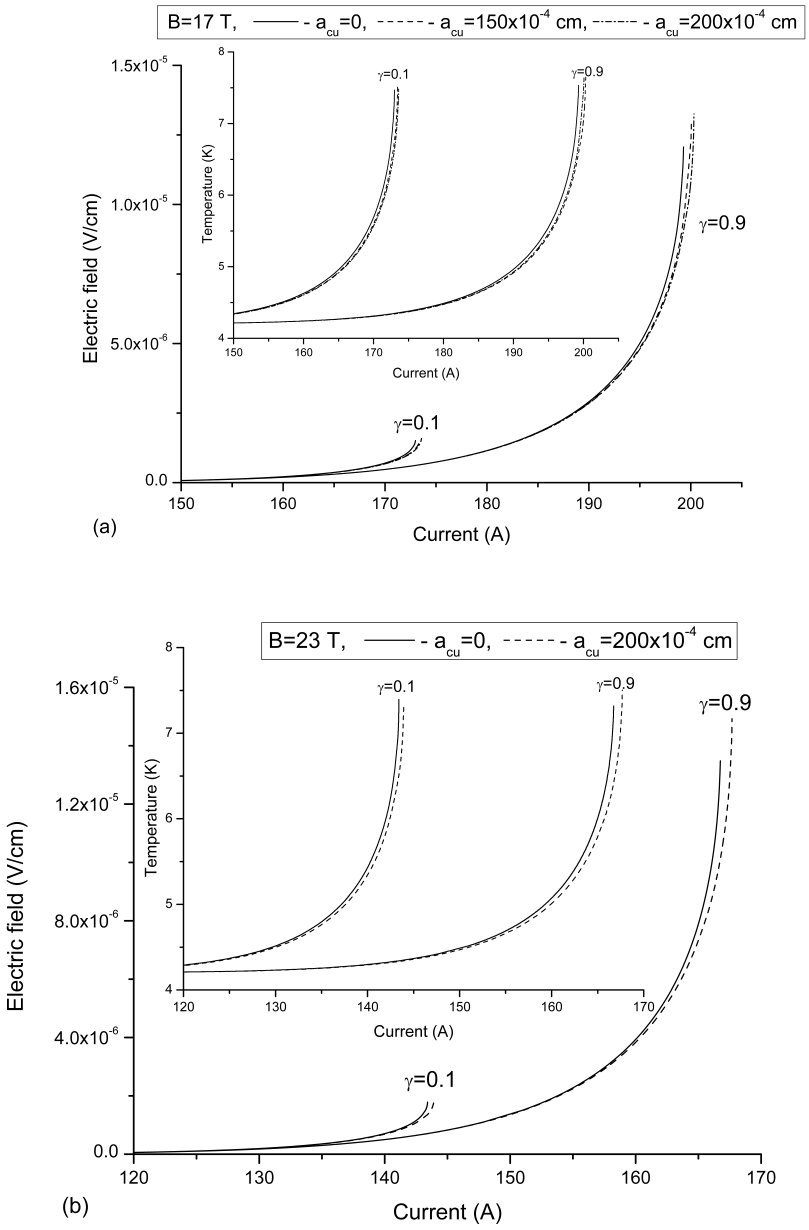

Fig. (3). The electric field and temperature in indirectly cooled Y123-tape as a function of charged current under different cooling conditions

when the voltage per unit length of tape induced in the superconductor and coatings satisfies the Kirchhoff's law in equation (2). In accordance with this law, the transport current is the sum of the currents flowing in the superconducting core J_s, silver J_{ag} and copper J_{cu} coatings, i.e., we arrive at the following equality

$$J = \eta_s J_s + \eta_{ag} J_{ag} + \eta_{cu} J_{cu} \tag{3}$$

Here, $E_c \sim 10^{-6}$ - 10^{-5} V/cm is a priory defined value of the electric field used in the determination of the critical current density $J_c(T,B)$; ρ_{ag} and ρ_{cu} are the specific electrical resistances of silver and copper, respectively; $\eta_s = a_s/a$, $\eta_{ag} = a_{ag}/a$ and $\eta_{cu} = a_{cu}/a$ are the volume fraction of superconductor, silver and copper, respectively; $q(T)$ is the heat flux to the coolant. In this section, we consider two cooling conditions, namely, conduction-cooling by cryocooler, which occurs at a constant heat transfer coefficient h according to [9], and cooling with LHe when the heat transfer is characterized by the presence of the nucleate and film boiling regimes. The corresponding dependences of $q(T)$ are written below.

Resistance dependences of silver and copper on the temperature and magnetic field for a given RRR = ρ(273 K)/ρ(4.2 K) were calculated according to the results presented in [10], which also gives the following values $\rho_{ag}(273\ \text{K}) = 1.48\times10^{-6}\ \Omega\times\text{cm}$ and $\rho_{cu}(273\ \text{K}) = 1.553\times10^{-6}\ \Omega\times\text{cm}$.

The critical current density $J_c(T,B)$ and the power law exponent $n(T,B)$ of the voltage-current characteristic of a superconductor as a function of temperature and magnetic field is generally non-linear. The calculated approximations of the required dependences $J_c(T,B)$ and $n(T,B)$ were based

on the theory developed in [11] and the data presented in [2] in which $J_c(T,B)$ and $n(T,B)$ were defined at $E_c = 10^{-5}$ V/cm.

Fig. (**2**) shows the corresponding temperature dependences of $\rho_{ag}(T,B)$, $\rho_{cu}(T,B)$, $J_c(T,B)$ and $n(T,B)$ on temperature calculated for the magnetic fields specified in the analysis made below.

The equations (2), (3) were transformed to the transcendental equation

$$\eta_s J_c(T,B)\left(\frac{E}{E_c}\right)^{1/n} = J - \left(\frac{\eta_{ag}}{\rho_{ag}} + \frac{\eta_{cu}}{\rho_{cu}}\right)E, \quad (4)$$

to determinate the electric field at a given current density. This equation is numerically solved in which the temperature was excluded taking into account that

$$q(T) = EJS / p \quad (5)$$

After this, the temperature is determined according to equation (5).

2.2. Current Instability Features of 2G Superconducting Tapes

Fig. (**3**) shows the typical voltage-current and temperature-current characteristics of the Y123-tape cooled initially to temperature T_0=4.2 K. The calculations were carried out at b=0.4 cm, $a_s = 2.25\times10^{-4}$ cm, $a_{ag} = 5\times10^{-4}$ cm and RRR=100 (for both silver and copper coatings) at different thickness of copper, cooling perimeter and external magnetic field. The presented curves correspond to the states occurring before the current instability. Analysis of the current-carrying capacity was made for the case when the cryocooler was used as a coolant. Correspondingly, the heat flux $q(T)$ was calculated as follows

$$q(T)=h(T - T_0) \quad (6)$$

in which the heat transfer coefficient is equal to $h=10^{-3}$ W/(cm^{2}K) according to [9].

As it is expected [12], for the given cooling condition, the current stability boundary follows from the equivalent conditions

$$\partial E/\partial J \to \infty \text{ or } \partial T/\partial J \to \infty \quad (7)$$

that allow one to find theoretically the instability parameters, namely, the current I_q, the electric field E_q and the temperature T_q beyond which HTS are unstable. The first of the conditions (7) is usually used in practice when n-value is large (n >30).

Note that the conditions (7) are the results of the static analysis. However, the boundary between stable and unstable states may be determined by other equivalent dynamic stability condition [12]. In real experiments the voltage-current and temperature-current characteristics are not static. Therefore, the stability boundary is also described by equalities $G(T_q, I_q)=W(T_q)$, $\partial G(T_q, I_q)/\partial T=\partial W(T_q)/\partial T$, which follow from the transient energy balance analysis. Here, $G(T)$ is the heat generation and $W(T)$ is the cooling power.

The respective values of the instability parameters are given in Tables **1 - 3**. Tables **4 - 7** contain the calculations of the limiting values of the current, the electric field and the temperature performed at b = 0.2 cm, $a_s = 10^{-4}$ cm, RRR = 100 and varying the thicknesses of the silver and copper coatings. In this case, the coolant temperature is assumed to be T_0 = 20 K.

The results presented lead to the following general conclusions.

First, the stabilizing effect of the thickness of the copper coating on the boundary of the current instability in the Y123-tape is practically absent under the indirect cooling conditions. This feature is a consequence of the fact that the main part of the transport current flows in the superconducting core even before the current instability (Fig. **4**). Therefore, small currents, which flow in silver and copper coatings before the instability, increase the instability current only slightly. As it will be proved below in section 3, this feature is caused by high values of the critical current of superconductor. However, the density of the current instability that is equal to $J_q=I_q/S$ decreases inversely proportional to the thickness of the copper coating. Accordingly, the engineering current density of tape is inevitably reduced under the indirect cooling conditions, if the amount of copper increases in the tape.

It should also be noted that the instability currents are reduced by approximately 20% in the indirect cooling when the coolant temperature increases from 4.2 K to 20 K according to the data given in Tables **4** and **6**. This result demonstrates the good possibility of the refrigerant temperature variation without significantly reducing the current stability boundary, which is certainly important when the operating temperature of the coil is set.

Second, the currents of instability are lower than the corresponding values of the critical current of the tapes ($I_q < I_c$) studied. At the same time, the electric field before the instability onset can be both subcritical ($E_q < E_c$) and overcritical ($E_q > E_c$). The latter regimes are established in the maximum possible value of the cooling tape perimeter. The importance of the existence of subcritical currents and the corresponding subcritical and overcritical electric fields should be highlighted. This result demonstrates that the critical parameters of superconductor, which are usually a priori defined, lead to the distorted estimations of the stable current range under the indirect cooling conditions. Therefore, to find correctly the boundaries of stable states, the non-isothermal nature of the formation of the voltage-current characteristics of Y123-tape should be taken into account, which occurs even in the stable stages despite the small currents flowing in the stabilizing layers. This conclusion is also important in the measuring of the critical currents of HTS.

Third, the currents of the instability approach the critical current of the tape under the improved cooling conditions of the tape. Moreover, as the numerical experiments show, these may be stable current modes when the permissible value of the current and the electric field will be overcritical ($I_q > I_c$, $E_q > E_c$) even under the indirect cooling conditions.

Table 1. Limiting stable Parameters at B=17 T, T_0=4.2 K, $a_{ag}=5\times10^{-4}$ cm, $I_c(T_0,B)$=233.0 A

γ=0.1			
a_{cu}, cm	**I_q, A**	**E_q, V/cm**	**T_q, K**
0	172.99	0.15143×10^{-5}	7.4685
50×10^{-4}	173.14	0.15907×10^{-5}	7.5942
100×10^{-4}	173.29	0.15835×10^{-5}	7.5404
150×10^{-4}	173.43	0.15870×10^{-5}	7.5103
200×10^{-4}	173.58	0.15912×10^{-5}	7.4823
γ=0.5			
a_{cu}, cm	I_q, A	E_q, V/cm	T_q, K
0	191.88	0.71447×10^{-5}	7.6212
50×10^{-4}	192.09	0.72095×10^{-5}	7.6133
100×10^{-4}	192.29	0.72894×10^{-5}	7.6128
150×10^{-4}	192.50	0.73575×10^{-5}	7.6069
200×10^{-4}	192.70	0.73996×10^{-5}	7.5892
γ=0.9			
a_{cu}, cm	I_q, A	E_q, V/cm	T_q, K
0	199.30	0.12490×10^{-4}	7.6512
50×10^{-4}	199.55	0.12676×10^{-4}	7.6636
100×10^{-4}	199.80	0.12811×10^{-4}	7.6621
150×10^{-4}	200.05	0.12908×10^{-4}	7.6508
200×10^{-4}	200.31	0.13255×10^{-4}	7.7006

Table 2. Limiting Stable Parameters at B=20 T, T_0=4.2 K, $a_{ag}=5\times10^{-4}$ cm, $I_c(T_0,B)$=212.41 A

γ=0.1			
a_{cu}, cm	**I_q, A**	**E_q, V/cm**	**T_q, K**
0	157.44	0.16754×10^{-5}	7.4911
50×10^{-4}	157.58	0.16796×10^{-5}	7.4617
100×10^{-4}	157.71	0.16785×10^{-5}	7.4225
150×10^{-4}	157.85	0.16819×10^{-5}	7.3929
200×10^{-4}	157.99	0.17315×10^{-5}	7.4510
γ=0.5			
a_{cu}, cm	**I_q, A**	**E_q, V/cm**	**T_q, K**
0	175.21	0.75680×10^{-5}	7.5089
50×10^{-4}	175.40	0.77244×10^{-5}	7.5339
100×10^{-4}	175.60	0.78977×10^{-5}	7.5765
150×10^{-4}	175.79	0.80171×10^{-5}	7.5901
200×10^{-4}	175.98	0.79150×10^{-5}	7.5107

γ=0.9			
a_{cu}, cm	**I_q, A**	**E_q, V/cm**	**T_q, K**
0	182.20	0.13265×10^{-4}	7.5506
50×10^{-4}	182.44	0.13528×10^{-4}	7.5795
100×10^{-4}	182.68	0.13738×10^{-4}	7.5946
150×10^{-4}	182.91	0.13769×10^{-4}	7.5657
200×10^{-4}	183.16	0.14240×10^{-4}	7.6440

Table 3. Limiting Stable Parameters at B=23 T, T_0=4.2 K, $a_{ag}=5\times10^{-4}$ cm, $I_c(T_0,B)$=193.84 A

γ=0.1			
a_{cu}, cm	**I_q, A**	**E_q, V/cm**	**T_q, K**
0	143.41	$0.17844'10^{-5}$	7.3931
$50'10^{-4}$	143.54	$0.17867'10^{-5}$	7.3607
$100'10^{-4}$	143.67	$0.17996'10^{-5}$	7.3474
$150'10^{-4}$	143.80	$0.18177'10^{-5}$	7.3438
$200'10^{-4}$	143.93	$0.18379'10^{-5}$	7.3438
γ=0.5			
a_{cu}, cm	**I_q, A**	**E_q, V/cm**	**T_q, K**
0	160.16	$0.81857'10^{-5}$	7.4717
$50'10^{-4}$	160.35	$0.82121'10^{-5}$	7.4455
$100'10^{-4}$	160.53	$0.82864'10^{-5}$	7.4387
$150'10^{-4}$	160.72	$0.83858'10^{-5}$	7.4419
$200'10^{-4}$	160.90	$0.85151'10^{-5}$	7.4565
γ=0.9			
a_{cu}, cm	**I_q, A**	**E_q, V/cm**	**T_q, K**
0	166.77	$0.14122'10^{-4}$	7.4651
$50'10^{-4}$	167.00	$0.14402'10^{-4}$	7.4933
$100'10^{-4}$	167.22	$0.14495'10^{-4}$	7.4786
$150'10^{-4}$	167.45	$0.14698'10^{-4}$	7.4892
$200'10^{-4}$	167.68	$0.14924'10^{-4}$	7.5046

Table 4. Limiting Stable Parameters at B=23 T, T_0=4.2 K, $a_{ag}=5\times10^{-4}$ cm, $I_c(T_0,B)$=39.15 A

γ=0.1			
a_{cu}, cm	**I_q, A**	**E_q, V/cm**	**T_q, K**
0	34.999	$0.10099'10^{-4}$	13.010
$20'10^{-4}$	35.048	$0.10123'10^{-4}$	12.956
$100'10^{-4}$	35.243	$0.10382'10^{-4}$	12.887

γ=0.5			
a_{cu}, cm	I_q, A	E_q, V/cm	T_q, K
0	41.747	$0.42422\cdot10^{-4}$	13.029
$20\cdot10^{-4}$	41.842	$0.43612\cdot10^{-4}$	13.207
$100\cdot10^{-4}$	42.228	$0.45963\cdot10^{-4}$	13.461
γ=0.9			
a_{cu}, cm	I_q, A	E_q, V/cm	T_q, K
0	44.549	$0.72487\cdot10^{-4}$	13.143
$20\cdot10^{-4}$	44.683	$0.74903\cdot10^{-4}$	13.377
$100\cdot10^{-4}$	45.234	$0.80864\cdot10^{-4}$	13.849

Table 5. Limiting Stable Parameters at B=23 T, T_0=4.2 K, $a_{ag}=30\times10^{-4}$ cm, $I_c(T_0,B)$=39.15 A

γ=0.1			
a_{cu}, cm	I_q, A	E_q, V/cm	T_q, K
0	35.130	$0.10253\cdot10^{-4}$	13.067
$20\cdot10^{-4}$	35.180	$0.10365\cdot10^{-4}$	13.089
$100\cdot10^{-4}$	35.378	$0.10702\cdot10^{-4}$	13.083
γ=0.5			
a_{cu}, cm	I_q, A	E_q, V/cm	T_q, K
0	42.170	$0.45863\cdot10^{-4}$	13.723
$20\cdot10^{-4}$	42.271	$0.46936\cdot10^{-4}$	13.873
$100\cdot10^{-4}$	42.682	$0.49741\cdot10^{-4}$	14.163
γ=0.9			
a_{cu}, cm	I_q, A	E_q, V/cm	T_q, K
0	45.243	$0.80969\cdot10^{-4}$	14.220
$20\cdot10^{-4}$	45.389	$0.83035\cdot10^{-4}$	14.409
$100\cdot10^{-4}$	45.997	$0.89796\cdot10^{-4}$	14.968

Table 6. Limiting Stable Parameters at B=23 T, T_0=20 K, $a_{ag}=5\times10^{-4}$ cm, $I_c(T_0,B)$=31.50 A

γ=0.1			
a_{cu}, cm	I_q, A	E_q, V/cm	T_q, K
0	27.978	$0.95332\cdot10^{-5}$	26.648
$20\cdot10^{-4}$	28.020	$0.97682\cdot10^{-5}$	26.755
$100\cdot10^{-4}$	28.183	$0.10187\cdot10^{-4}$	26.816
γ=0.5			
a_{cu}, cm	I_q, A	E_q, V/cm	T_q, K
0	33.455	$0.41200\cdot10^{-4}$	26.871
$20\cdot10^{-4}$	33.536	$0.41895\cdot10^{-4}$	26.935
$100\cdot10^{-4}$	33.867	$0.44293\cdot10^{-4}$	27.123

γ=0.9			
a_{cu}, cm	**I_q, A**	**E_q, V/cm**	**T_q, K**
0	35.731	$0.70312\cdot10^{-4}$	26.958
$20\cdot10^{-4}$	35.846	$0.71259\cdot10^{-4}$	27.004
$100\cdot10^{-4}$	36.322	$0.77140\cdot10^{-4}$	27.391

Table 7. Limiting stable parameters at B=23 T, T_0=20 K, $a_{ag}=30\times10^{-4}$ cm, $I_c(T_0,B)$=31.50 A

γ=0.1			
a_{cu}, cm	**I_q, A**	**E_q, V/cm**	**T_q, K**
0	28.084	$0.98305\cdot10^{-5}$	26.797
$20\cdot10^{-4}$	28.124	$0.98480\cdot10^{-5}$	26.752
$100\cdot10^{-4}$	28.291	$0.10404\cdot10^{-4}$	26.906
γ=0.5			
a_{cu}, cm	I_q, A	E_q, V/cm	T_q, K
0	33.786	$0.43188\cdot10^{-4}$	27.184
$20\cdot10^{-4}$	33.871	$0.43752\cdot10^{-4}$	27.225
$100\cdot10^{-4}$	34.220	$0.46865\cdot10^{-4}$	27.526
γ=0.9			
a_{cu}, cm	I_q, A	E_q, V/cm	T_q, K
0	36.269	$0.75682\cdot10^{-4}$	27.508
$20\cdot10^{-4}$	36.392	$0.76670\cdot10^{-4}$	27.558
$100\cdot10^{-4}$	36.903	$0.82908\cdot10^{-4}$	27.976

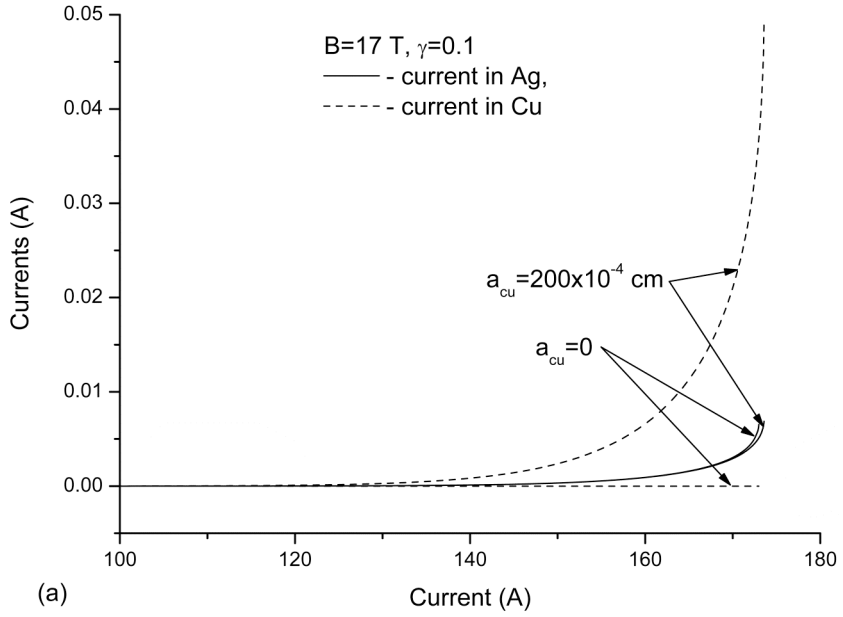

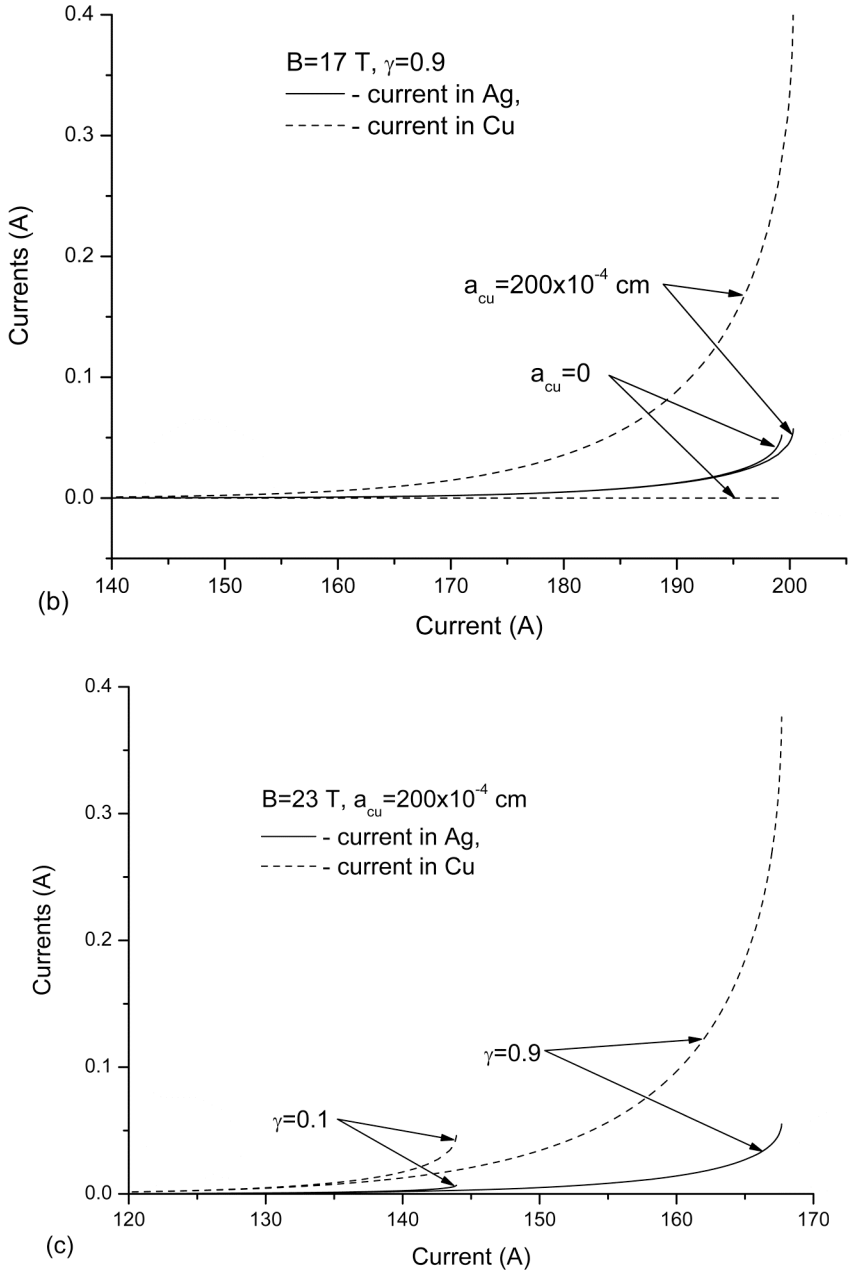

Fig. (4). Current sharing between the stabilizing layers.

Their existence is also dependent on the properties of the superconductor and the stabilizing coating. In particular, stable overcritical regimes of the Y123-tape that take place under the LHe cooling condition are discussed below. A detail analysis of the subcritical and the overcritical regimes at a constant value of the heat transfer coefficient is made in section 3.

Fourth, the instability currents decrease and the corresponding values of the electric field increase with increasing magnetic field. Thus, the instability current will be knowingly characterized at high magnetic fields by the subcritical instability current. In this case, the induced electrical voltages can be both subcritical and overcritical. For practical applications, this fact is very important when the diagnosis of unstable current regimes based on the determination of the allowable operating current by measuring of the limiting stable level of voltages is carried out.

Let us now estimate the current-carrying properties of the Y123-tape cooled by LHe because of its high critical properties that allow the superconducting coils generating a high magnetic field up to 30 T [2] to be created. An analysis of the limiting current-carrying capacity was carried out at b=1 cm, a_s=10^{-4} cm, a_{ag}=5×10^{-4}cm, T_0=4.2 K, RRR=100 varying the thickness of the copper layer and the induction of an external magnetic field. In this case, we assume that the cooling perimeter is equal to $p=b+2(a_s+a_{ag}+a_{cu})$. As above, the critical current density and n-value were calculated according to [11]. Their temperature dependences at B = 30 T are shown in Fig. (**2**). The values of $q(T)$ assuming an

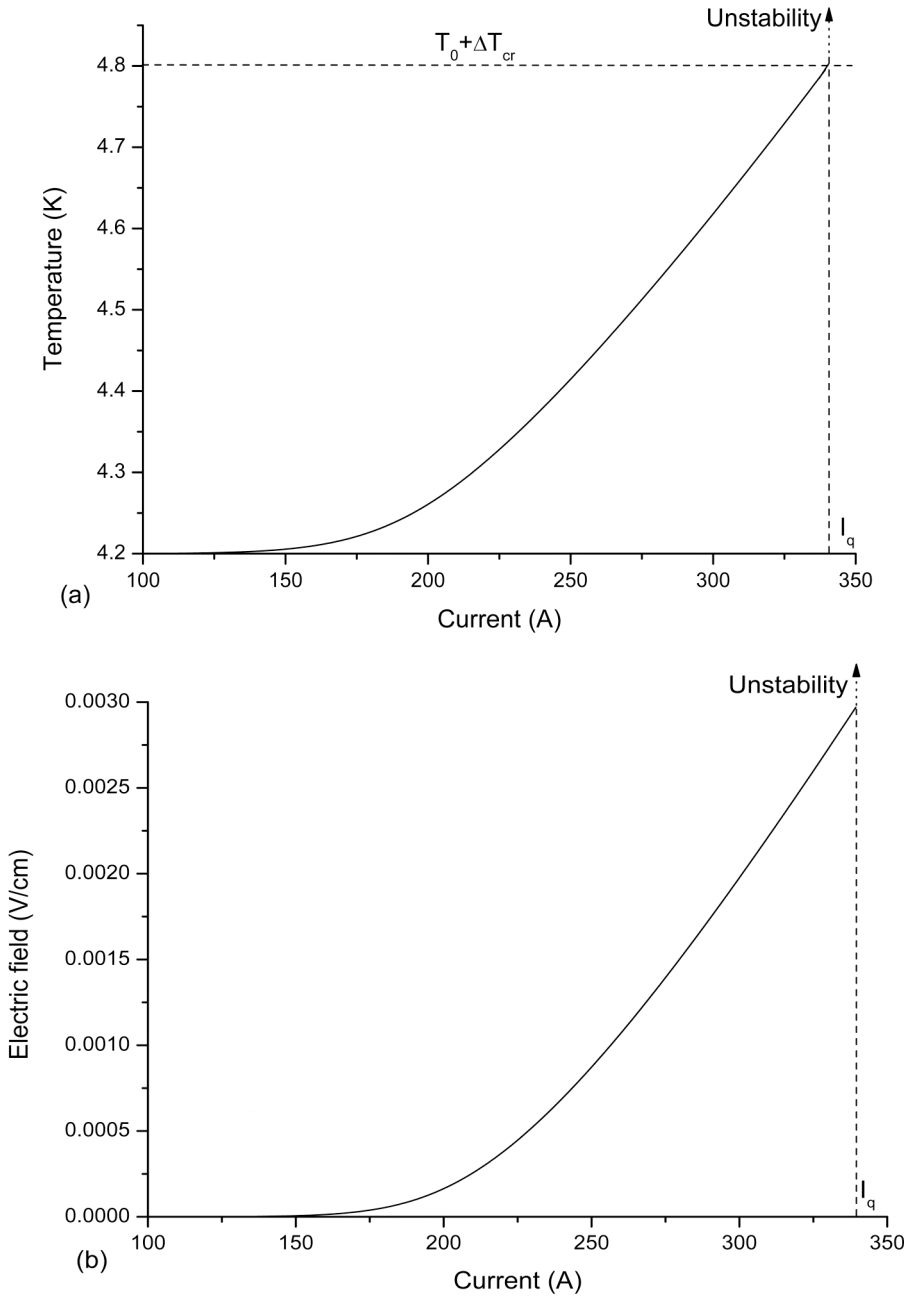

Fig. (5). Permissible rise in the temperature and the electric field in the Y123-tape cooled by the LHe at B = 30 T, RRR=100, a_{ag}=10^{-4}cm, T_0=4.2 K.

abrupt transition from nucleate to film boiling regime [13] are written according to [14] as

$$q(T)[W/cm^2] = \begin{cases} 2.15(T-T_0)^{1.5}, & T-T_0 < \Delta T_{cr} = 0.6K \\ 0.06(T-T_0)^{0.82}, & T-T_0 \geq \Delta T_{cr} = 0.6K \end{cases} \quad (8)$$

where ΔT_{cr} is the overheating temperature above which the transition from the nucleate boiling regime to the film one takes place.

Fig. (**5**) shows the temperature-current and voltage-current characteristics of tape, calculated for the nucleate cooling condition that exists in the temperature range from T_0 to T_0+ΔT_{cr}. Under the approximation used, the overheating of tape, which becomes higher than ΔT_{cr}, leads to its transition to the film boiling mode that corresponds to the stability boundary as it will be an irreversible increase in temperature of the tape [15]. In other words, the stability of current states will be violated after a trivial overheating over ΔT_{cr}. The corresponding stability boundary is shown in Fig. (**5**) by dotted lines. The results of the stability analysis of the Y123-tape with variable thickness of the copper coating are shown in Figs. (**6-8**). They lead to the following conclusions.

Current instability in the LHe-cooled Y123-tape occurs at overcritical values of the electric field and the current. As a result, the electric field before the instability exceeds more than by two orders a priori set the critical electric field of superconductor. (The later is equal to E_c=10^{-5} V/cm). Accordingly, the currents of the instability essentially exceed the critical currents during cooling of tape by LHe. For

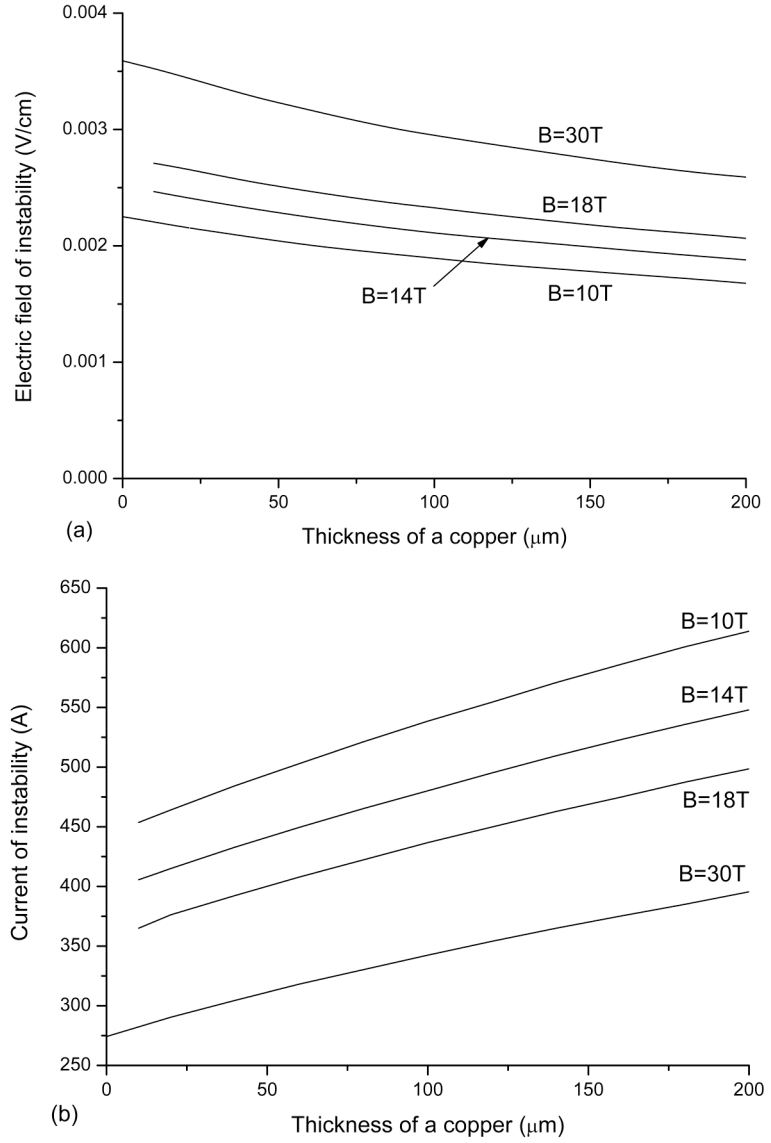

Fig. (6). The limiting electric fields and currents depending on the thickness of the copper coating.

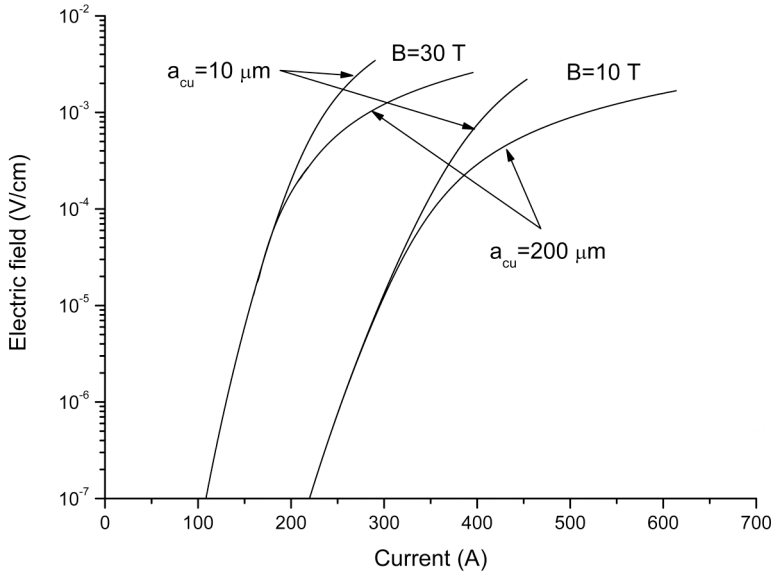

Fig. (7). Effect of the current sharing on the voltage-current characteristic of the Y123-tape.

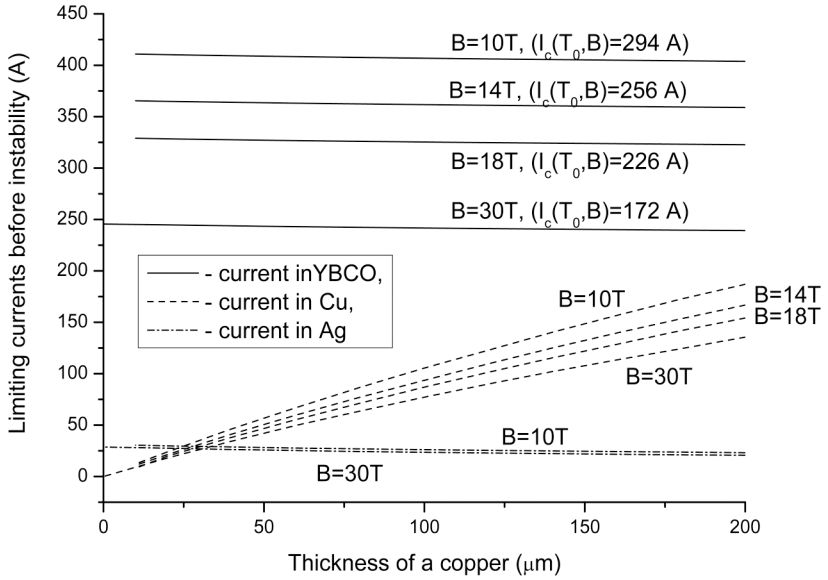

Fig. (8). The influence of the copper coating thickness on the limiting currents in the superconductor and stabilizing layers.

example, the critical current of the tape investigated is equal to 226 A at B = 18 T. As it can be seen from Fig. (**6**), this value is smaller than the currents of the instability even in the ultrahigh magnetic field B = 30 T. Note also that the instability current is approximately 140% of the critical current of tapes in this magnetic field at a_{cu}=200 μm.

The increase in the copper coating thickness leads to almost linear increase in the instability current in the whole investigated range of the magnetic field. However, despite this feature the respective values of the electric field decrease. This is a direct consequence of the mechanism of current sharing between the superconductor and the stabilizing layers. Figs. (**7** and **8**) demonstrate these features. They clearly show that the copper coating plays the main role in this mechanism. Note, first, that noticeable current sharing happens in the overcritical electric field range (Fig. **7**). In other words, undesirable heat generations are small due to the voltage-current characteristic of superconductor in the subcritical voltage range. Second, currents in the silver layer are almost not changed with the increase in its thickness but the current increase in copper is about 0.7 A per 1 μm copper layer at 30 T. This rise in the instability current increases on decreasing external magnetic field. Nevertheless, the main part of transport current flows in the superconductor before the instability onset. Therefore, the total heat generation in the tape will slightly increase, if the amount of copper in tape increases.

It is also important to emphasize that the presented results demonstrate the existence of the characteristic value of the copper coating thickness after which its role in the current stability is the most noticeable. For the tape considered, this stabilizing effect is carried out at $a_{cu} > 50$ μm.

In conclusion, let us compare the above discussed stability conditions of the Y123-tape with different cooling modes. They show that the layers of the superconducting coil cooled with LHe will have different stabilizing level. Indeed, the outer layers that are intensively cooled with LHe will be stabilized better than its inner ones for which the cooling conditions are close to the indirect cooling. This fact should be taken into account in terms of ensuring effective cooling conditions of multi-section superconducting magnets that will generate high magnetic field.

2.3. The Effect of Size on the Current Instability of 2G Tapes

The results discussed above were formulated under the assumption that the distribution of the temperature would be uniform in the cross section of a tape. Let us investigate the peculiarities of the formation of the thermal and electric states of 2G tapes taking into account the non-uniform temperature distribution in the cross section. To understand the physical features of this problem, let us find the static temperature distribution in the two tapes under consideration, for which all geometrical parameters are written above and presented in Fig. (**1**). Here, the cross section changes in the range $0 < y < a = a_s + a_{ag} + a_{cu}$. Assume also that the condition $b >> a$ takes place; the tapes are in the mode of fully penetrated current; the surface y=0 of the tapes is thermally insulated and the heat exchange occurs only on the surface $y=a$. Accordingly, using the finite difference method let us find the solution of the following one-dimensional boundary problem

$$\frac{d}{dy}\left[\lambda_s(T)\frac{dT_s}{dy}\right] + EJ_s = 0, \tag{9}$$

$$\frac{d}{dy}\left[\lambda_{ag}(T)\frac{dT_{ag}}{dy}\right] + EJ_{ag} = 0, \tag{10}$$

$$\frac{d}{dy}\left[\lambda_{cu}(T)\frac{dT_{cu}}{dy}\right] + EJ_{cu} = 0 \tag{11}$$

under the conditions

$$\frac{dT_s}{dy} = 0, \quad y = 0, \tag{12}$$

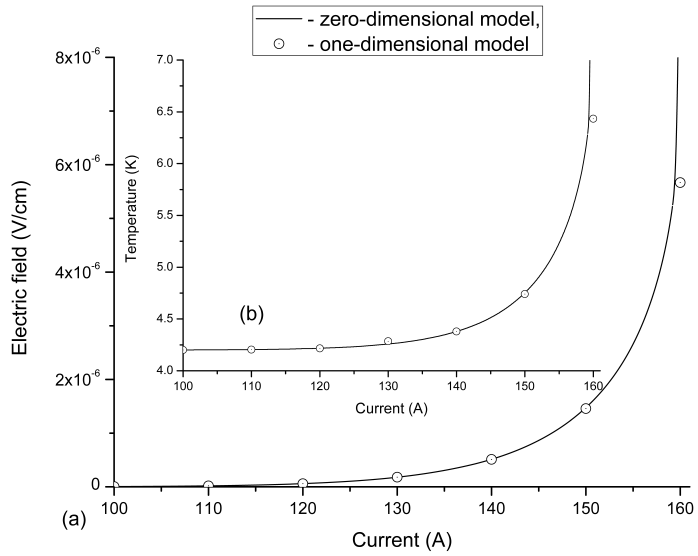

Fig. (9). Voltage-current (a) and temperature-current (b) characteristics of indirectly cooled Y123-tape

$$T_s = T_{ag}, \quad \lambda_s(T)\frac{dT_s}{dy} = \lambda_{ag}(T)\frac{dT_{ag}}{dy}, \quad y = a_s, \tag{13}$$

$$T_{ag} = T_{cu}, \quad \lambda_{ag}(T)\frac{dT_{ag}}{dy} = \lambda_{cu}(T)\frac{dT_{cu}}{dy}, \quad y = a_s + a_{ag} \tag{14}$$

$$\lambda_{cu}(T)\frac{dT_{cu}}{dy} + q(T) = 0, \quad y = a_s + a_{ag} + a_{cu} \tag{15}$$

and the Kirchhoff's relations (2) and (3). Here, T_s, T_{ag} and T_{cu} are the cross section temperature in the superconductor, silver and copper, respectively; λ_s, λ_{ag} and λ_{cu} are the thermal conductivities of superconductor, silver and copper, respectively; $q(T)$ is the heat flux to the coolant. As above, let us consider two cooling conditions, namely, the conduction-cooling and cooling with LHe. Correspondingly, the value of $q(T)$ is defined by the formula (6) in the first cooling mode and according to the formula (8) in the second cooling mode.

The calculations were also made in the zero-dimensional approximations to compare results of different approaches. In these cases, it was assumed that the cooling perimeter p of tapes is equal to b according to the boundary problem defined by equations (9) – (15).

The stability investigation was made at B = 23 T and h=10^{-3} W/(cm^{2}K). The dependences of $\rho_{ag}(T,B)$, $\rho_{cu}(T,B)$, $J_c(T,B)$ and $n(T,B)$ used in calculations are shown in Fig. (**2**). The resistivities of silver and copper were also used in the calculations of their thermal conductivities according to the Wiedemann-Franz law for RRR=100. The thermal conductivity of Y123 was approximated by the formula

λ_s [W/(cm×K)] =-0.016906+0.109355T-9.47339×$10^{-05}$$T^2$-1.2475×$10^{-05}$$T^3$+6.00586×$10^{-08}$$T^4$, T < 90 K

in accordance with results presented in [16].

Fig. (**9**) presents the voltage-current and the temperature-current characteristics of the tape discussed above under the conduction-cooling conditions at T_0=4.2 K. It is seen that the current instability is a result of the conditions

$$\partial E/\partial I \to \infty \text{ or } \partial T/\partial I \to \infty \tag{16}$$

that describe the stability boundary in the non-uniform distribution of the charged current. However, difference between the analysis of the boundary of current stability is practically absent in the zero-dimensional and one-dimensional approximations. This feature is due to the fact that the temperature distribution in the tape is practically uniform, as seen from Fig. (**10**). As a result, all peculiarities discussed above using zero-dimensional approximation will take place in multi-dimensional models. This conclusion simplifies essentially the stability analysis, which should be made for HTS devices.

Fig. (**11**) shows the temperature-current and the voltage-current characteristics calculated at B = 30 T for the above-investigated tape cooled by the LHe. As in the zero-dimensional approach, the current instability onset is initiated by the transition from the nucleate to the film boiling regime (Fig. **12**). However, difference between zero-dimensional and one-dimensional approximations is more noticeable than in the conduction-cooling conditions. This is a result of the non-uniform temperature distribution in this cooling mode, as it follows from Fig. (**12**). This feature leads to an additional conduction flux, which plays stabilizing role. Therefore, the one-dimensional approximation will give more optimistic estimations in the current stability conditions of Y123-tapes cooled by LHe. Moreover, this cooling mode is also characterized by noticeable stabilizing role of copper layer (Fig. **13**). As a result, the stable current sharing will lead to the essential increase in the current stability boundary in the overcritical regimes. This feature demonstrates excellent electrodynamics stabilization of Y123-tapes cooled by LHe in the high magnetic field.

2.4. Conclusion: Operating Conditions of 2G Tapes

The main peculiarities of the formation of stable thermal and electric states in superconducting current-carrying elements made on the basis of Y123 have been investigated, taking into account the variation in the thicknesses of the

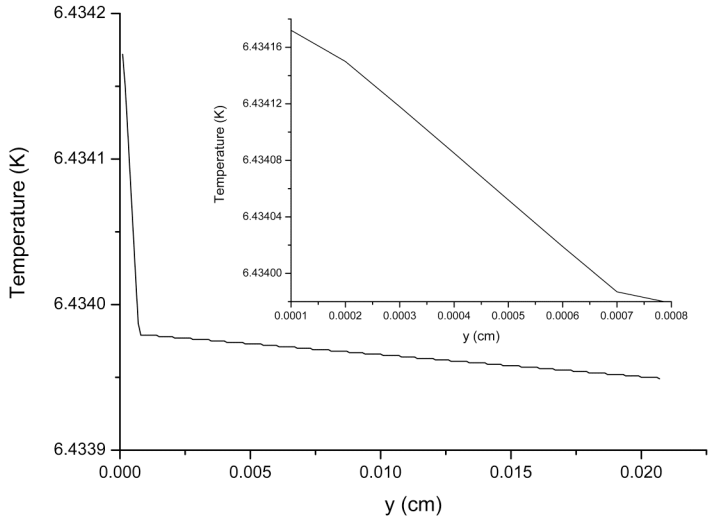

Fig. (10). Temperature distribution in the cross section of indirectly cooled Y123-tape.

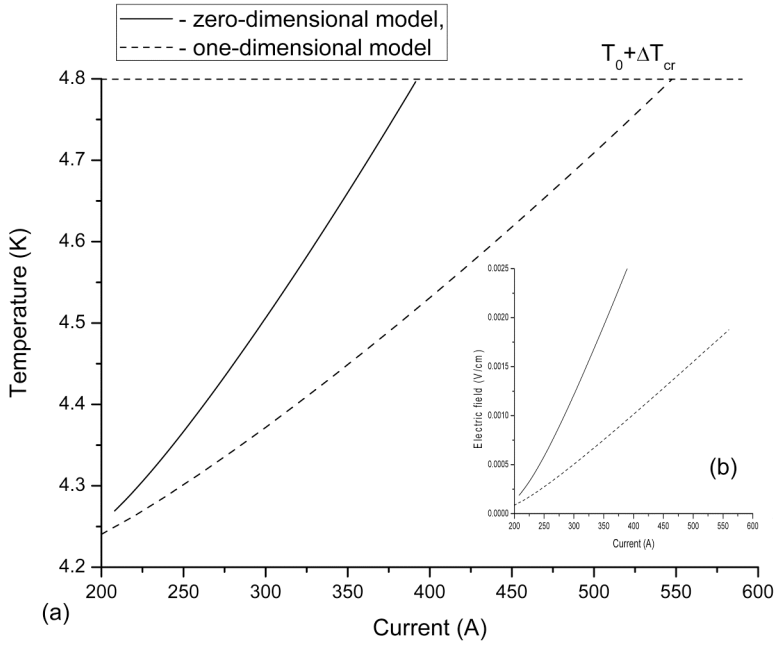

Fig. (11). Temperature-current (a) and voltage-current (b) characteristics of LHe cooled Y123-tape.

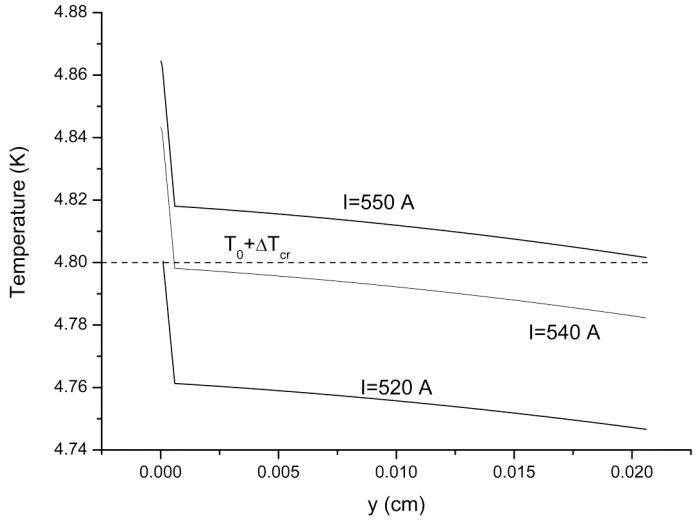

Fig. (12). Temperature distribution in the cross section of LHe cooled Y123-tape.

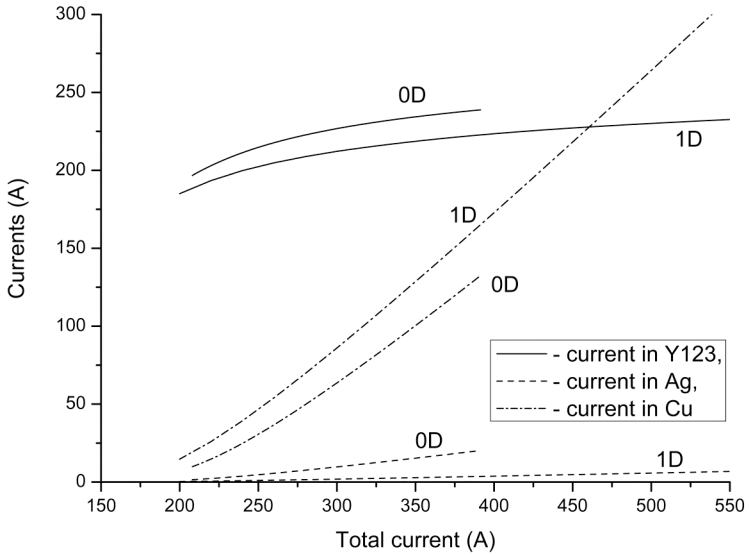

Fig. (13). Current sharing in the LHe cooled Y123-tape calculated in the framework of zero-dimensional (0D) and one-dimensional (1D) approximations.

copper and silver coatings, external magnetic field and the cooling conditions. The analysis of the current instability conditions of Y123-tapes shows that:

1. The copper and silver coatings do not affect the limiting allowable values of the currents stably charged into the Y123-tape I the conduction-cooling conditions. Thus, they do not have the stabilizing effect on the Y123-tape electrodynamics stability of the charged currents at these cooling regimes.

2. Currents of the instability increase almost linearly with increasing thickness of the copper layer in the Y123-tape cooled by the LHe. This feature is due to a stable current sharing between the superconductor and the copper coating, if its thickness exceeds the characteristic value.

3. Instability conditions of stable current states of Y123-tapes can lead to both subcritical and overcritical regimes.

4. The design of a superconducting magnet, which will use cryocooler as a coolant, must take into account that the instability onset may occur when the operating current is smaller than the critical current of the tape.

5. Current stability analysis of superconducting magnets, which will use the LHe as a coolant, show that they will have overcritical stability conditions even in the zero-dimensional approximation. The one-dimensional analysis leads to more optimistic estimations.

6. The inner layers of superconducting coil cooled by the LHe are in less favorable stability conditions than the outer part of coil.

3. INSTABILITY OF CURRENTS CHARGED INTO HTS SUPERCONDUCTING COMPOSITE (MULTI-FILAMENT SUPERCONDUCTING CORE IN NON-SUPERCONDUCTING MATRIX)

Progress in the technology of 1G superconducting composites has opened new ways for the creation of high-T_c superconducting devices [17, 18]. They promise as many potential applications as the low-temperature superconducting composites. Currently, the production of long-length HTS composites, which can be used in a variety of superconducting devices, is arranged. For example, the superconducting current-carrying elements on the basis of bismuth ceramics are reached the critical current densities required for the practical use of them when the coolant temperature can be easily obtained by cryocooler. However, it is necessary to define conditions of the electrodynamics stabilization, which will provide stability boundary of the charged current. Below-performed analysis was made to formulate the criteria of the current instabilities of HTS composites considering the thermal prehistory of them during the formation of stable states.

3.1. Zero-Dimensional Model of Superconducting Composite

In order to perform the analytical investigation of the features inherent to formation of the stable current regimes of HTS composites, let us use the zero-dimensional static approximation. Let us also assume that superconducting filaments would have the small transverse dimension that would not lead to the magnetic instabilities; the superconductor uniformly distributed over the cross section of a composite with the volume fraction of η ($0 < \eta < 1$) and an continuous medium approximation can be used; the critical current density of the superconductor $J_c(T,B)$ as a function of temperature is approximated by the linear relationship at the given magnetic field; n-value of voltage-current characteristic of a superconductor does not depend on the temperature and magnetic field.

Under these assumptions, the temperature of the composite cooled by cryocooler can be determined by solving the heat balance equation (1) with relation (6). In this case, the transport current with density J is the sum of the currents flowing in the superconducting core J_s and matrix J_m

$$J = \eta J_s + (1-\eta) J_m \qquad (17)$$

and the electric field induced in the superconductor and the matrix with resistivity ρ_m, is described by equations

$$E = E_c\left[J_s / J_c(T,B)\right]^n = J_m\rho_m(T,B) \tag{18}$$

Here, according to the assumptions made above

$$J_c(T,B) = J_{c0}(B)\frac{T_{cB}(B)-T}{T_{cB}(B)-T_0} \tag{19}$$

where J_{c0} and T_{cB} are the known critical current density and temperature of superconductor in a given magnetic field.

Note that the parameters, which were not mentioned here, have the same physical meaning as parameters used above in section 2.

The problem defined by equations (1), (17) - (19) allows one to find the criteria that describe the stability boundary of the superconducting state of HTS composite when the limiting current may be charged.

3.2. Linear Theory of Current Instability

Rewrite equations (17) and (18) in the form

$$E = E_c\left\{\frac{J - E(1-\eta)/\rho_m(T,B)}{\eta J_c(T,B)}\right\}^n \tag{20}$$

Eliminate the temperature from this equality using equation (1), taking into account the linear temperature dependence of the critical current density (19) and assuming that $\rho_m(T,B)\approx\rho_m(T_0,B)$=const according to Fig. (**2**). Then the non-isothermal current-voltage characteristic of the superconducting composite can be written as

$$J = \frac{\eta J_{c0}\left(\frac{E}{E_c}\right)^{1/n} + \frac{1-\eta}{\rho_m}E}{1+\frac{\eta J_{c0}SE}{hp(T_{cB}-T_0)}\left(\frac{E}{E_c}\right)^{1/n}} \tag{21}$$

This expression is easily transformed to the following relation

$$J = \eta J_{c0}\frac{\left(E/E_c\right)^{1/n} + E/E_\eta}{1+\left(E/E_h\right)\left(E/E_c\right)^{1/n}} \tag{22}$$

where $E_\eta = \dfrac{\eta J_{c0}\rho_m}{1-\eta}$, $E_h = \dfrac{hp(T_{cB}-T_0)}{\eta J_{c0}S}$. Accordingly, an increase of composite temperature can be calculated as

$$T = T_0 + (T_{cB}-T_0)\frac{\left(E/E_c\right)^{1/n} + E/E_\eta}{\left(E/E_c\right)^{1/n} + E_h/E} \tag{23}$$

Values of E_η and E_h define the characteristic values of the electric field, whose influence on the growth of voltage-current characteristic of the superconducting composite in the zero-dimensional approximation. Indeed, it is easy to find that the main part of the charged current will flow in the superconducting core of the composite, if $E << E_c\left(E_\eta / E_c\right)^{n/(n-1)}$. At the same time, the voltage-current characteristic is close to the isothermal one ($T \sim T_0$), if $E << E_c\left(E_h / E_c\right)^{n/(n+1)}$. Typical values E_η and E_h depend on the properties of the superconductor and matrix, heat exchange conditions. Accordingly, they can satisfy both $E_\eta << E_h$ and $E_\eta >> E_h$ conditions. In the first case, the current sharing between the superconductor and matrix will have of an isothermal character, while the non-isothermal states will take place under the second condition. In particular, let us estimate their possible values assuming that $\rho_m \sim 10^{-7}$ Ω×cm, $J_{c0} \sim 10^5$ A/cm^2, $p \sim 0.1$ cm, $S \sim 10^{-2}$ cm^2, $\eta \sim 0.5$, T_{cB}-$T_0 \sim 20$ K. Then $E_\eta \sim 10^{-2}$ V/cm and $E_h \sim 4\times10^{-6}$ V/cm in the cooling, which occur when the cryocooler is used as a coolant ($h \sim 10^{-3}$ W/(cm^{2}K)). Therefore, in the analysis of the voltage-current characteristics in these cooling modes, the appropriate temperature difference between the temperature of the composite and cooler should be considered.

The values E_η and E_h makes it possible to redefine a so-called Stekly parameter, which is equal to [19, 20]

$$\alpha = \frac{\eta^2 J_{c0}^2\rho_m S}{hp(1-\eta)(T_{cB}-T_0)} \tag{24}$$

It is known that the physical meaning of this dimensionless parameter is the ratio of a characteristic value of the volumetric power of Joule heat release in the matrix to the characteristic value of the volumetric capacity of the heat flow to the coolant. At the same time, it is easy to find that $\alpha = E_\eta / E_h$. In other words, the Stekly parameter is also the ratio of the characteristic values of the electric field, above which the current sharing between the superconductor and the matrix occurs to the characteristic value of the electric field separating the isothermal state from the non-isothermal one. Since it is usually $\alpha >> 1$ ([19, 20]) then one must take into account the non-isothermal nature of the electric state formation in the superconducting composites under this condition.

The prescribed relations permit the conditions of the current instability in composite superconductors to be found. According to the conditions (7), one can find the limiting stable values of the electric field E_q, current I_q and temperature T_q. They satisfy the following relations

$$\begin{aligned}&\frac{\eta}{n}\frac{J_{c0}}{E_c^{1/n}}E_q^{(1-n)/n} - \left(\eta J_{c0}/E_c^{1/n}\right)^2\\ &\frac{S}{hp(T_{cB}-T_0)}E_q^{2/n} = \frac{1-\eta}{\rho_m}\left[\frac{\eta}{n}\frac{J_{c0}}{E_c^{1/n}}\frac{S}{hp(T_{cB}-T_0)}E_q^{(n+1)/n} - 1\right],\end{aligned} \tag{25}$$

$$I_q = \frac{\eta\frac{J_{c0}}{E_c^{1/n}}E_q^{1/n} + \frac{1-\eta}{\rho_m}E_q}{1+\frac{J_{c0}}{E_c^{1/n}}\frac{\eta S}{hp(T_{cB}-T_0)}E_q^{(n+1)/n}}S, \tag{26}$$

$$T_q = T_0 + (T_{cB}-T_0)\frac{\eta + \frac{1-\eta}{\rho_m}\frac{E_c^{1/n}}{J_{c0}}E_q^{(n-1)/n}}{\eta + \frac{hp(T_{cB}-T_0)}{S}\frac{E_c^{1/n}}{J_{c0}}E_q^{-(n+1)/n}} \tag{27}$$

Let us introduce the dimensionless variables $\varepsilon_q = E_q/E_c$, $i_q = J_q/(\eta J_{c0})$, $\theta_q = (T_q-T_0)/(T_{cB}-T_0)$. Then the expressions (25) – (27) are transformed to

$$\frac{1}{n\varepsilon_2}\varepsilon_q^{1+\frac{1}{n}}+\frac{\varepsilon_1}{\varepsilon_2}\varepsilon_q^{\frac{2}{n}}-\frac{\varepsilon_1}{n}\varepsilon_q^{\frac{1}{n}-1}=1, \quad (28)$$

$$i_q=\frac{\varepsilon_q^{1/n}+\varepsilon_q/\varepsilon_1}{1+\varepsilon_q^{1+\frac{1}{n}}/\varepsilon_2}, \quad (29)$$

$$\theta_q=\frac{\varepsilon_q^{1+\frac{1}{n}}+\varepsilon_q^2/\varepsilon_1}{\varepsilon_q^{1+\frac{1}{n}}+\varepsilon_2} \quad (30)$$

where $\varepsilon_1=E_\eta/E_c$, $\varepsilon_2=E_h/E_c$.

Let us use the obtained relationships and evaluate the effect of the properties of the matrix, the critical current of the superconductor and the volume fraction coefficient on the current instability conditions. As an example, let us define the limiting stable currents charged into the superconducting composite based on Bi2212/Ag in a silver matrix placed in the external magnetic field B = 10 T and cooled by cryocooler (h=10^{-3} W/(cm^{2}K), T_0 = 4.2 K). Varying the values RRR, J_{c0} and η, let use the following parameters E_c =10^{-6} V/cm, S=0.0123 cm^2, p=0.47 cm, T_{cB}=26.1 K, n=11 corresponding to the composite investigated in [21]. In this case, the resistivity of silver as a function of temperature and magnetic field will be approximated according to [10], as it was made above.

Fig. (**14**) shows the results of the calculation of the limiting values of the electric field, current and temperature as a function of the volume fraction coefficient of the composite at different RRR and J_{c0} values. First, it is seen that there exist subcritical stability conditions ($E_q < E_c$, $I_q < I_c$). They appear at the high values of the volume fraction coefficient after exceeding of some value of the critical current density of the superconductor. Second, in a wide range of η - variation, it may take place the overcritical regimes of stability ($E_q > E_c$, $I_q > I_c$) leading to the noticeable composite overheating. For example, the overcritical regimes will exist at small values of the η even when J_{c0} is high. Third, there exist intermediate stability regimes when the stability boundary is characterized by overcritical values of the electric fields but subcritical currents. In particular, as follows from Fig. (**14**), similar modes occur when η is varying from 0.4 to 0.7, if J_{c0} = 10^5A/cm^2.

The existence of stable regimes is also depending on the external magnetic field. Numerical experiments show that the stability states will tend to the subcritical regimes with increasing external magnetic field in a wide range of η - variation.

An important conclusion that follows from Fig. (**14**) should be emphasized. It is seen that the current-carrying capacity of superconducting composite degrades with increasing volume fraction coefficient or the critical current density. In other words, the currents of the instability do not increase proportionally to the increase of the critical current of the composite. This feature occurs both under overcritical and subcritical stability conditions.

The effect of the degradation is caused by non-isothermal nature of the formation of the electrodynamics states of the composite, i.e., with the inevitable difference of the superconducting composite temperature from the coolant temperature before the instability. As it follows from relation (12), the effect of temperature on the formation of the superconducting state is explained by the thermal influence term that is equal to $\frac{\eta J_{c0} SE}{hp(T_{cB}-T_0)}\left(\frac{E}{E_c}\right)^{1/n}$. It leads to the corresponding increase in the deviation of the non-isothermal voltage-current characteristics of the composite on those calculated in the isothermal approximation. Accordingly, as discussed above, increase in the volume fraction coefficient or the critical current density will lead to the rise of the thermal influence term and, thus, to the thermal degradation of the current-carrying capacity of the composite. Besides, the effect of thermal degradation will occur with the decreasing temperature margin of superconductor ΔT=T_{cB} – T_0 or the heat transfer conditions. The increase in the composite cross section will be also accompanied by the degradation of the current-carrying capacity. It should be noted that this feature takes place at h=const because T_q is not constant due to the existence of the thermal influence term.

The influence of the matrix resistance on the limiting stable values of the electric field, current and temperature of the superconducting composite is shown in Fig. (**15**). The calculations were carried out at J_{c0}=1.52×10^4A/cm^2, different values of the heat transfer coefficient and η. It proves to be that the stable overcritical regimes will exist under the intensive cooling conditions or in composites with small resistivity of the matrix. Furthermore, depending on the values of η or h, there exist stability regions in which variation of RRR can influence significantly the stability conditions of the charged current. These modes are typical of composites having a relatively low value of the volume fraction coefficient. The probability of their occurrence increases with the improvement in the heat exchange conditions. In these cases, the allowable increase in the electric field and the temperature is high. Namely, the allowable overheating can exceed 10 K due to the overcritical values of the induced electric field. Therefore, it must account for the corresponding change in the temperature dependences of the properties of the superconductor and the matrix when the stability conditions are analyzed in these states. This result can also be taken into account when the critical properties of the superconductor are measured because it is believed a priori that the temperature of the composite is equal to the temperature of the coolant.

Thus, it has been proved that the current stability conditions of the high-temperature superconducting composite can also be subcritical and overcritical at h=const. However, it should be noted that the instability parameters E_q, I_q and T_q depend on the ratio $J_{c0}/E_c^{1/n}$ as it follows from (25) – (27). This ratio is constant for the power voltage-current characteristic of superconductor at n=const and T=T_0. Therefore, if the values of J_{c0} and E_c are arbitrarily chosen in the isothermal part of the power voltage-current characteristic of superconductor, then E_q, I_q and T_q do not depend on the arbitrary choice of coupled values of (J_{c0}, E_c).

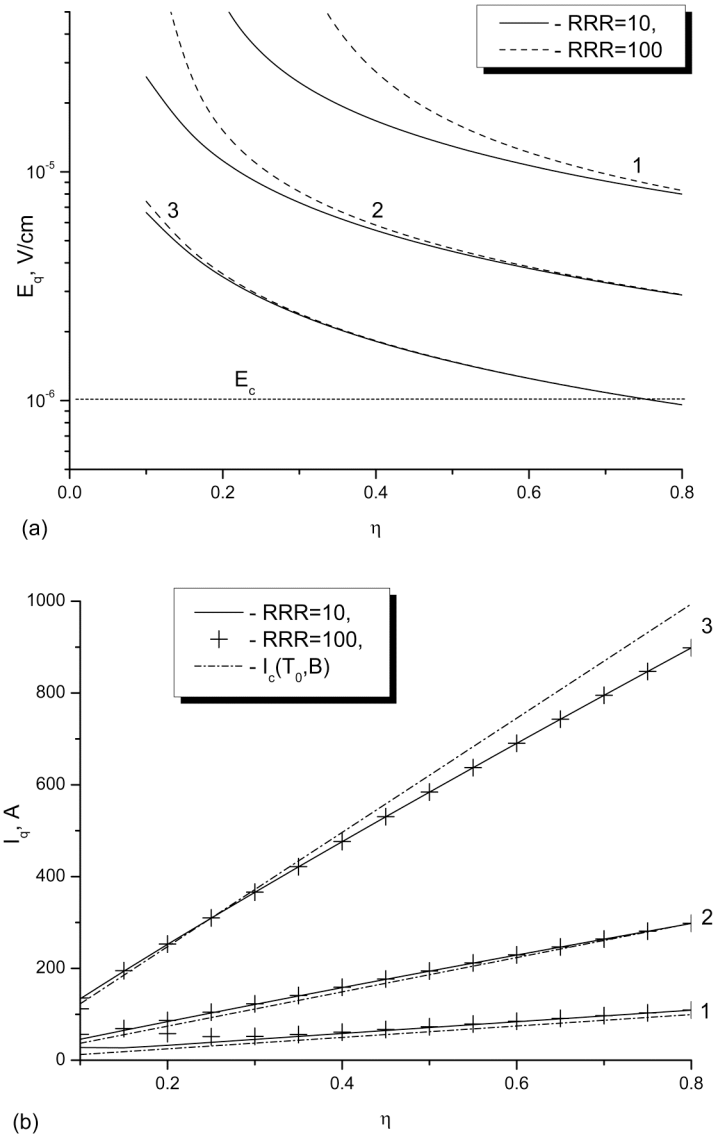

Fig. (14). Limiting values of the electric field (**a**), current (**b**) and temperature (**c**) as functions of volume fraction coefficient: 1 - $J_{c0} = 10^4$ A/cm^2; 2 - $J_{c0} = 3x10^4$ A/cm^2; 3 - $J_{c0} = 10^5$ A/cm^2.

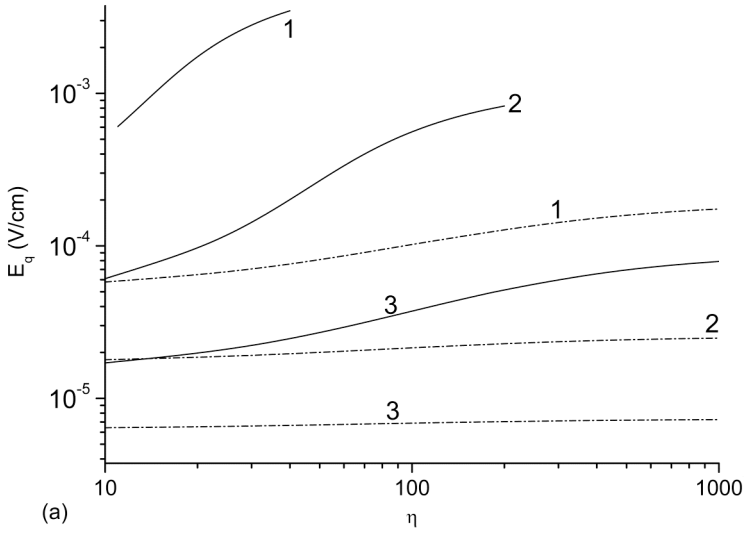

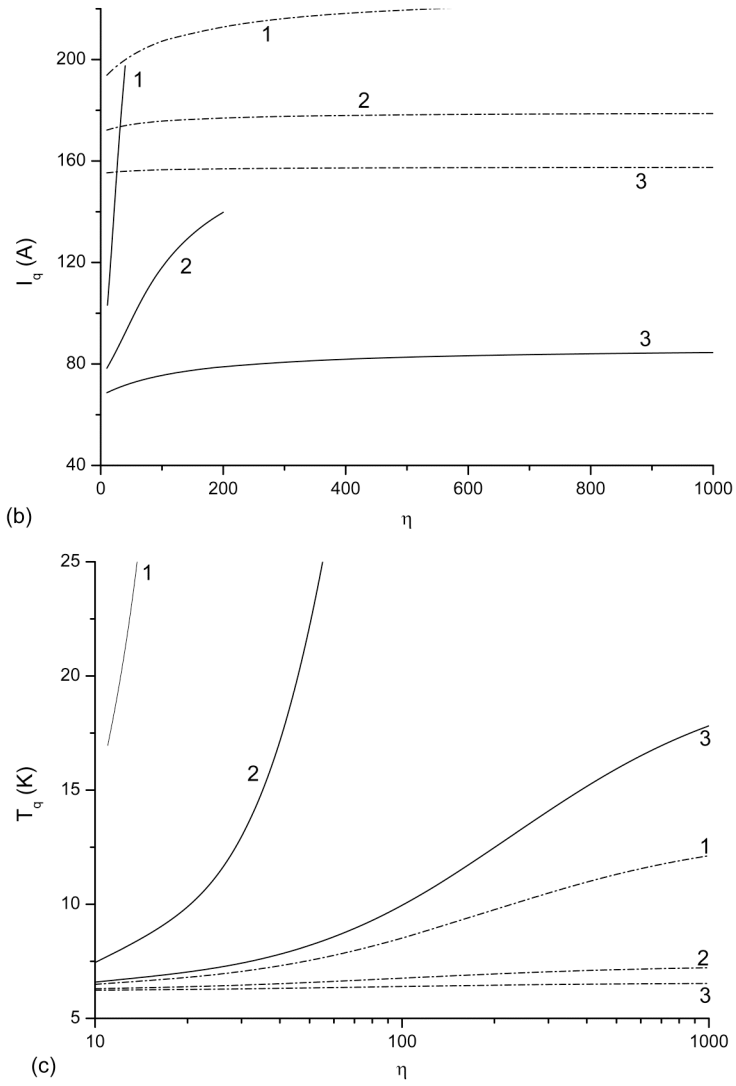

Fig. (15). Effect of matrix resistance on the limiting values of the electric field (a), current (b) and temperature (c): 1 - $h = 10^{-2}$ W/(cm^{2}K); 2 - $h = 3\text{x}10^{-3}$ W/(cm^{2}K); 3 - $h = 10^{-3}$ W/(cm^{2}K); - • - η = 0.2; - η = 0.5.

At the same time, the arbitrary choice of (J_{c0}, E_c) will lead to the existence of sub- and overcritical stable states.

Let us write the criteria of their existence in the framework of the considered zero-dimensional approximation ($hS/\lambda p << 1$). Taking $\varepsilon_q = 1$, it is easy to find the boundary between the subcritical and the overcritical values of the electric field. In this case, the parameters of composite must satisfy equality $\varepsilon_2 = (1+n\varepsilon_1)/(\varepsilon_1+n)$. For a given value of ε_2, the corresponding current of the instability is

$$i_q = \frac{n}{n+1} + \frac{1}{(n+1)\varepsilon_1} \tag{31}$$

i.e., it is certainly less than the critical current of composite. Then the current instability occurs in the subcritical region ($E_q < E_c$, $I_q < I_c$), if the condition

$$\frac{\eta J_{c0} E_c S}{hp(T_{cB} - T_0)} > \frac{\eta\rho_m J_{c0} + n(1-\eta)E_c}{n\eta\rho_m J_{c0} + (1-\eta)E_c} \tag{32}$$

takes place. In these cases, the thermal stability parameter satisfies to the condition

$$\alpha > 1 + \frac{\varepsilon_1^2 - 1}{\varepsilon_1 n + 1} \tag{33}$$

If these conditions are violated, then the stable electric field exceeds the critical E_c. However, in this case, as has been discussed above, the charged currents can be both subcritical and overcritical. The latter ($i_q > 1$) exists, when $\varepsilon_q > \varepsilon_{q,v}$, where the value of $\varepsilon_{q,v}$ follows from the solution of equation

$$\varepsilon_1 = \varepsilon_{q,v}^{1/n} + \varepsilon_{q,v} - \alpha\varepsilon_{q,v}^{1+(1/n)} \tag{34}$$

Accordingly, the possible stable states of high-temperature superconducting composites will be characterized by overcritical values of the electric fields and the subcritical currents when the condition

$$\frac{\eta J_{c0} E_c S}{hp(T_{cB} - T_0)} < \frac{\eta\rho_m J_{c0} + n(1-\eta)E_c}{n\eta\rho_m J_{c0} + (1-\eta)E_c} \tag{35}$$

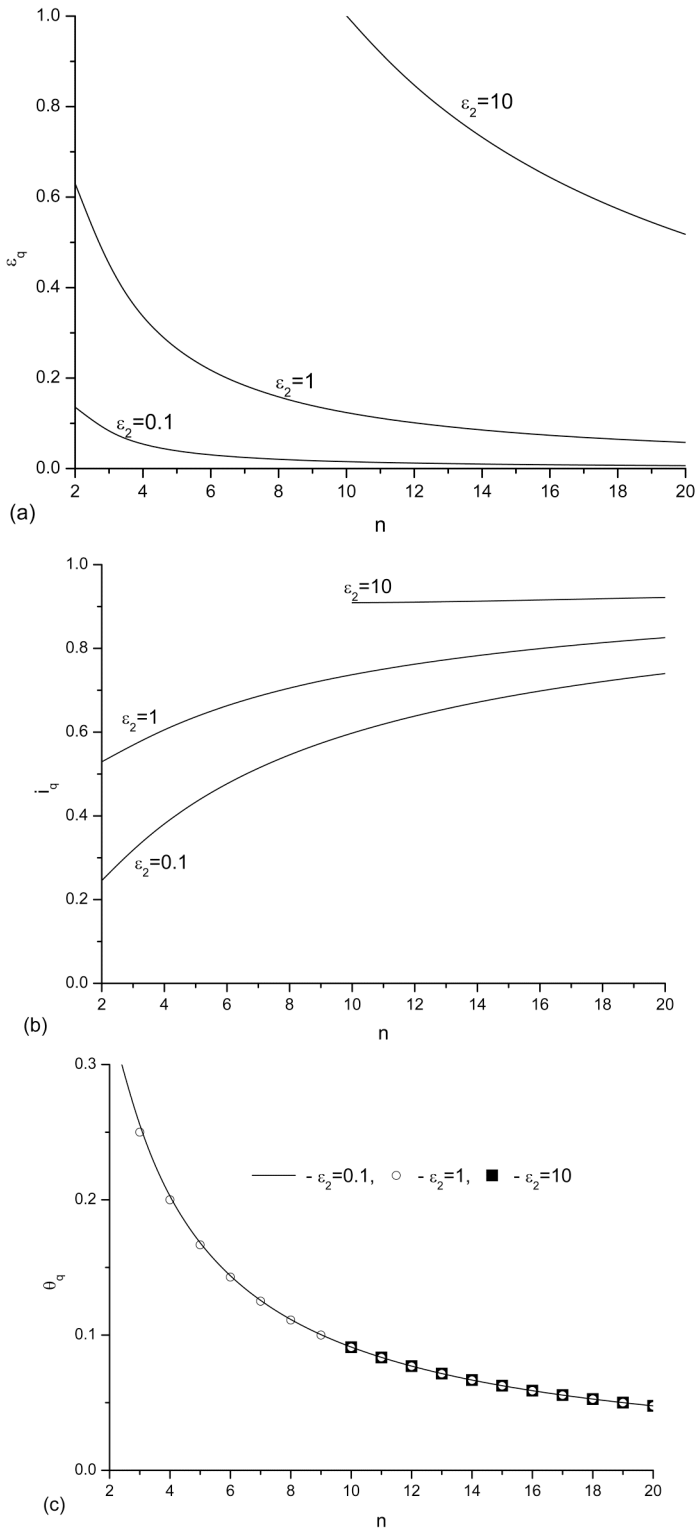

Fig. (16). Effect of nonlinearity of the voltage-current characteristic on the maximum allowable values of the electric field (a), current (b) and temperature (c).

takes place.

The calculation results of the subcritical and overcritical regimes in dimensionless terms introduced above are shown in Figs. (**16** and **17**). They were obtained at $\varepsilon_1=10^4$, which is a typical value of high-temperature superconducting composite according to the above estimate. Fig. (**16**) shows the effect of n - value on the allowable subcritical stable values of the electric field, current and temperature calculated for different values of ε_2. According to (28) – (30), it is easy to obtain the following estimates

$$\varepsilon_q \sim \left(\frac{\varepsilon_2}{n}\right)^{\frac{n}{n+1}}, \quad i_q \sim \frac{n}{n+1}\left(\frac{\varepsilon_2}{n}\right)^{\frac{1}{n+1}} \tag{36}$$

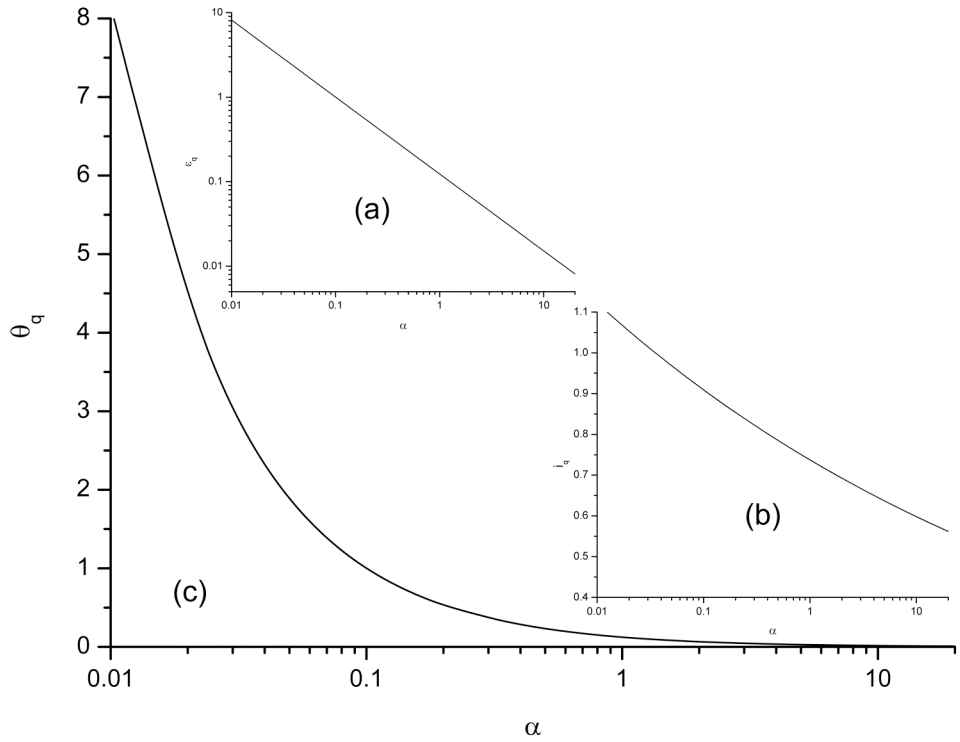

Fig. (17). The dependence of the limiting values of the electric field (**a**), current (**b**) and temperature (**c**) on the stability parameter at n=10.

for a given range of admissible parameters. Accordingly, if the superconductor's quality deteriorates, that is, n-value decreases, the conditions of the current stability will be characterized by the high values of permissible overheating of superconducting composites.

On the whole, the results presented in Fig. (**16**) lead to the conclusion which is important for practical applications. It turns out that the stably charged current and induced electric field not only can be below the critical values of E_c and J_{c0} but lead to the finite overheating depending on the n - value. This feature of the thermal formation of superconducting composite states should be taken into account when the critical parameters of a superconductor are experimentally determined, since permissible operating temperature of superconductor cannot be equal to the coolant temperature even in the subcritical region.

The influence of the stability parameter α on the values of the electric field and the current before instability is presented in Fig. (**17**). It should be noted that, in the framework of the performed dimensionless analysis, the α-variation is caused by a change in the values ε_2 due to the corresponding change in the heat transfer conditions on the surface of the composite, namely, in the term hp/S. Fig. (**17**) demonstrates that the flux creep plays a positive role in the stabilization of the operating regimes of high-temperature superconducting composites. Indeed, according to the existing thermal stability theory [19, 20], there exists the condition of the complete thermal stabilization ($\alpha < 1$) under which charged currents exceeding the critical current of a superconductor will flow stably only in the matrix. At the same time, the stability conditions of real high-temperature superconducting composites may be both subcritical and overcritical at $\alpha < 1$. In other words, high-temperature superconducting composites with the voltage-current characteristics taking into account flux creep have better thermal stability conditions as the charged current may flow both in superconductor and matrix at $\alpha < 1$. Accordingly, the transport current will flow only in the matrix when the condition takes place according to relations (22) and (23). Therefore, the approximation based on the concept of the fixed critical current of a superconductor will lead to more severe current stability conditions.

$$\left(\frac{\eta J_{c0}}{E_c^{1/n}}\right)^2\left[\frac{S}{hp(T_{cB}-T_0)}\right]^{1-\frac{1}{n}}\left(\frac{\rho_m}{1-\eta}\right)^{1+\frac{1}{n}} < 1 \qquad (37)$$

In conclusion, it should be pointed out that the linear zero-dimensional approximation discussed in this section may be used in the current stability investigation of Y123-coated tapes. To do this, one must use the following substitutions

$$\eta = \eta_s,$$

$$\frac{1-\eta}{\rho_m} = \frac{\eta_{ag}}{\rho_{ag}} + \frac{\eta_{cu}}{\rho_{cu}}$$

in all written formulae. Accordingly, the characteristic values of the electric field, calculated above, may be written as follows

$$E_\eta = \frac{\eta_s J_{c0}}{\dfrac{\eta_{ag}}{\rho_{ag}} + \dfrac{\eta_{cu}}{\rho_{cu}}}, \quad E_h = \frac{hp(T_{cB}-T_0)}{\eta_s J_{c0} S}$$

Therefore, in particular, the current sharing mechanism between superconductor and stabilizing layers will not take place under the condition

$$E << E_c \left\{ \eta_s J_{c0} / \left[E_c \left(\frac{\eta_{ag}}{\rho_{ag}} + \frac{\eta_{cu}}{\rho_{cu}} \right) \right] \right\}^{n/(n-1)}$$

Thereby, the higher the value J_{c0} (the critical current density of superconductor at operating temperature) or the thickness of superconductor, the higher the probability of the regimes in which the total part of the charged current will flow in superconductor. The latter formula also allows one to write the estimation $a_{ag}/\rho_{ag} << a_{cu}/\rho_{cu}$ according to which the copper layer will play the main role in the current sharing mechanism.

3.3. Conclusion: Operating Conditions of 1G Wires

The analysis performed shows that the non-isothermal formation of the stable current states of HTS composites and conditions of their electrodynamics stability are characterized by the following features.

1. There are the characteristic values of the electric field, which allow one to estimate the role of heat transfer conditions and the current sharing mechanism between the superconductor and the matrix in the shaping of a stable state of HTS composites.

2. It is proved that the limiting stable values of the electric field and the current can be both subcritical and overcritical at constant value of heat transfer coefficient. The corresponding criteria defining their boundaries are written. The existence of the subcritical and the overcritical stable regimes is dependent on the properties of the superconductor and matrix, heat exchange conditions with a coolant. In particular, the subcritical modes will be observed in the composites with high volume fraction of superconductor, under the non-intensive cooling conditions or high magnetic fields. Stable overcritical regimes of current states of superconducting composites will take place at small values of the volume fraction of superconductor or the thermal stabilization parameter ($\alpha < 1$). These overcritical regimes are characterized by the high stable overheating of the composite.

3. The critical values of the electric field and the current, which are usually a priori defined, do not describe the boundary of stable states. Therefore, these values do not have the physical sense according to which they determine the critical parameters of the superconductor.

4. The inevitable overheating of the composite before the instability leads to the thermal degradation of its current-carrying capacity. Therefore, the currents of the instability do not increase in proportion to the critical currents of HTS. The effect of degradation affects essentially the stability conditions that take place at subcritical regimes.

CONFLICT OF INTEREST

The authors confirm that this article content has no conflicts of interest.

ACKNOWLEDGEMENT

The work was carried out under the project of the Russian Foundation for Basic Research with number 12-08-00261-a.

REFERENCES

[1] Bird MD, Bole S, Eyssa YM. Test results and potential for upgrade of the 45 T hybrid insert. IEEE Trans Appl Supercond 2000; 10: 439-42.

[2] Watanabe K, Nishijima G, Awaji S, *et al*. Compact design of a 30 T superconducting magnet incorporating $YBa_2Cu_3O_7$ coated conductor tapes and pre-reacted Nb_3Sn strand cables. Appl Phys Express 2008; 1: 101703.

[3] Watanabe K, Awaji S, Nishijima G, *et al*. Cryogen-free 23 T superconducting magnet with a 7.5 T $YBa_2Cu_3O_7$ insert coil. Appl Phys Express 2009; 2: 113001.

[4] Watanabe K, Motokawa M. Cryogen-free high field superconducting magnets. IEEE Trans Appl Supercond 2000; 10: 489 - 492.

[5] Watanabe K, Nishijima G, Awaji S, *et al*. Performance of a cryogen-free 30 T-class hybrid magnet. IEEE Trans Appl Supercond 2006; 16: 934-7.

[6] Burgoyne JW, Daniels PD, Timms KW, *et al*. Advances in superconducting magnets for commercial and industrial applications IEEE Trans Appl Supercond 2000; 10: 703-6.

[7] Newson MS, Ryan DT, Wilson MN, *et al*. Progress in the design and operation of high-Tc coils using dip-coat BSCCO-2212/Ag tape. IEEE Trans Appl Supercond 2002; 12: 725-8.

[8] Stautner W, Sivasubramaniam K, Laskaris ET, *et al*. A Cryo-free 10 T high-field magnet system for a novel superconducting application. IEEE Trans Appl Supercond 2011; 21: 2225-8.

[9] Bellis RH, Iwasa Y. Quench propagation in high-T_c superconductors. Cryogenics 1994; 34: 129-44.

[10] Seeber B. Handbook of Applied Superconductivity. Editor B. Seeber. Bristol: IOP Publishing 1998; vol. 1: p. 1067-82.

[11] Inoue M, Kiss T, Mitsui D, *et al*. Current transport properties of 200 A-200 m-class IBAD YBCO coated conductor over wide range of magnetic field and temperature. IEEE Trans Appl Supercond 2007; 17: 3207-3210.

[12] Romanovskii VR, Watanabe K. Basic formation peculiarities of the stable and unstable states of high-T_c composite superconductors at applied fully penetrated currents. Physica C 2005; 425: 1 - 13.

[13] Altov VA, Zenkevich VB, Kremlev MG, and Sychev VV. Stabilization of Superconducting Magnetic Systems. New York: Plenum Press 1977.

[14] Brentari EG, Smith RV. Nucleate and film pool boiling design correlation for O_2, N_2, H_2 and He. Int Adv Cryog Eng 1965; 10: 325-41.

[15] Romanovskii VR, Watanabe K, Awaji S, *et al*. Current-carrying capacity dependence of composite $Bi_2Sr_2CaCu_2O_8$ superconductor on the liquid coolant conditions. Supercond Sci Technol 2006; 19: 703-10.

[16] Uher C. Thermal conductivity of high-T_c superconductors. J Supercond Nov Magn 1990; 3: 337-50.

[17] Larbalestier D, Gurevich A, Feldmann DM. High-T_c superconducting materials for electric power applications. Nature 2001; 414: 368-77.

[18] Malozemoff AP, Verebelyi DT, Fleshler S, *et al*. HTS wire: status and prospects magnets. Physica C 2003; 386: 424-30.

[19] Wilson MN. Superconducting magnets. Oxford: Clarendon Press 1983.

[20] Gurevich AV, Mints RG, Rakhmanov AL. The physics of composite superconductors. NY: Begell House 1997.

[21] Seto T, Murase S, Shimamoto S, *et al*. Thermal stability of Ag/B2212 tape at cryocooled condition. Cryog Eng 2001; 36: 60-7.

Received: July 10, 2013 Revised: September 05, 2013 Accepted: September 13, 2013

© Romanovskii *et al.*; Licensee *Bentham Open*.

This is an open access article licensed under the terms of the Creative Commons Attribution Non-Commercial License (http://creativecommons.org/licenses/by-nc/3.0/), which permits unrestricted, non-commercial use, distribution and reproduction in any medium, provided the work is properly cited.